Photodetachment, photofragmentation, and fragment autodetachment of $[O_{2n}(H_2O)_m]^-$ clusters: Core-anion structures and fragment energy partitioning

Daniel J. Goebbert and Andrei Sanov[a)]
Department of Chemistry, University of Arizona, Tucson, Arizona 85721-0041, USA

(Received 23 June 2009; accepted 17 August 2009; published online 11 September 2009)

Building on the past studies of the O_{2n}^- and $O_2^-(H_2O)_m$ cluster anion series, we assess the effect of the strong hydration interactions on the oxygen-core clusters using photoelectron imaging and photofragment mass spectroscopy of $[O_{2n}(H_2O)_m]^-$ ($n=1-4$, $m=0-3$) at 355 nm. The results show that both pure-oxygen and hydrated clusters with $n \geq 2$ form an O_4^- core anion, indicated in the past work on the pure-oxygen clusters. All clusters studied can be therefore described in terms of $O_4^-(H_2O)_m(O_2)_{n-2}$ structures, although the O_4^- core may be strongly perturbed by hydration in some of these clusters. Fragmentation of these clusters yields predominantly O_2^- and $O_2^-(H_2O)_l$ ($l<m$) anionic products. The low-electron kinetic energy O_2^- autodetachment features, prominent in the photoelectron images, signal that the fragments are vibrationally excited. The relative intensity of photoelectrons arising from O_2^- fragment autodetachment is used to shed light on the varying degree of fragment excitation resulting from the cluster fragmentation process depending on the solvent conditions. © *2009 American Institute of Physics*. [doi:10.1063/1.3224135]

I. INTRODUCTION

Superoxide O_2^- and its clusters O_{2n}^- or $O_2^-(H_2O)_m$ are known for their complex and rich photochemistry, which is due to a large number of low lying electronic states that arise from the open-shell configurations of both O_2 and O_2^-.[1–15] The above cluster types have been studied extensively using a variety of experimental techniques, including mass spectrometry,[16] photofragment action, and translational spectroscopy,[3,5,8] as well as photoelectron spectroscopy.[2,6,9,11,12] Most studies have focused either on the oxygen clusters, O_{2n}^-,[2,3,6–11] or hydrated superoxide, $O_2^-(H_2O)_m$.[4,5,12] The experiments on O_{2n}^- have demonstrated the formation of O_4^-, which has been invoked as a core anion representing a structurally distinct species within these clusters.[17] Given the small dissociation energy of O_4^- (0.455 eV),[18] it is of interest whether its identity is preserved under hydration, which is characterized by strong ionic hydrogen-bonding interactions, often well in excess of the above dissociation energy of O_4^-. This is one of the questions addressed in the present work, investigating cluster anions of the type $[O_{2n}(H_2O)_m]^-$ by photoelectron imaging and photofragment spectroscopy.

Early on, Arshadi and Kebarle[16] obtained hydration energies for superoxide clusters in the gas- phase from equilibrium measurements. Other groups[1,6,18,19] have reported solvation energies of superoxide with oxygen. The experiments showed that water binding energies to superoxide are significantly larger than corresponding oxygen binding energies. In particular, the water binding energy to O_2^- in the $O_2^-(H_2O)$ complex is evaluated at 0.967 ± 0.065 eV,[12] arising from favorable ion-dipole interaction. In comparison, the binding energy of oxygen to superoxide to form O_4^- is 0.455 ± 0.22 eV.[18] While smaller than the hydration energy, the O_2 binding energy to O_2^- is nonetheless substantially larger than what one might expect for purely electrostatic (charge-induced-dipole or charge-quadrupole) interactions within a solvated $O_2^- \cdot O_2$ complex. This binding energy is, in fact, characteristic of the weakly covalent character of O_4^-, in which the excess electron is believed to be equally shared between two O_2 moieties.[2,9,12,20,21] It significantly exceeds any subsequent oxygen binding energies in larger O_{2n}^- clusters, suggesting their $O_4^-(O_2)_{n-2}$ structures. Selected binding energies from previous studies are summarized in Table I.

Hydrated superoxide cluster anions, $O_2^-(H_2O)_m$, have also been studied.[5,12,15] In the photodissociation of $O_2^-(H_2O)_m$, $m \leq 33$, examined over the range of 200–300 nm, Lavrich *et al.*[5] observed two different anionic pathways: dissociation of the O_2^- core to form atomic oxygen anion and dehydration. The dehydration channel was found to favor longer wavelengths and larger clusters, while O_2^- dissociation dominated at shorter wavelengths and in smaller clusters. Luong *et al.*[12] studied the dissociative photodetachment reactions for $O_2^-(H_2O)_m$, $m=1-6$ at 388 and 258 nm. Their photoelectron spectra indicated a decrease in solvation energies for $m>4$, suggesting that the first solvation shell around O_2^- consists of four water molecules. An infrared study of $O_2^-(H_2O)_nAr_m$ clusters also concluded the first solvation shell of O_2^- consisted of four water molecules.[22]

The photoelectron and fragmentation spectra of O_{2n}^- have similarly been measured[2,6–11] with a particular focus on the photochemistry of O_4^-.[6–9,11] DeLuca *et al.*[2] examined the photofragmentation of O_{2n}^-, $n=2-6$, at 1064 nm and observed the formation of both O_2^- and O_4^-. They also measured the photoelectron spectra of O_{2n}^-, $n=2-6$ at 355 nm, all of which, with the exception of O_2^-, consisted of broad vibra-

a)Electronic mail: sanov@u.arizona.edu.

TABLE I. $O_{2n}^-(H_2O)_m$ cluster dissociation energies.

Reaction	Energy (kJ/mol)	Energy (eV)	Reference
$O_4^- \rightarrow O_2^- + O_2$	43.9 ± 2.1	0.455	18
$O_6^- \rightarrow O_4^- + O_2$	10.5 ± 0.8	0.109	18
$O_8^- \rightarrow O_6^- + O_2$	10.0 ± 0.8	0.104	18
$O_2^-(H_2O) \rightarrow O_2^- + H_2O$	93.3 ± 6.3	0.967	12
$O_2^-(H_2O)_2 \rightarrow O_2^-(H_2O) + H_2O$	72.0 ± 4.2	0.746	16
$O_2^-(H_2O)_3 \rightarrow O_2^-(H_2O)_2 + H_2O$	64.4 ± 4.2	0.667	16
$O_6^-(H_2O) \rightarrow O_4^- + H_2O$	65.3[a]	0.677	This work
$O_4^-(H_2O)_2 \rightarrow O_4^-(H_2O) + H_2O$	67.2[a]	0.696	This work
$O_4^-(H_2O)_3 \rightarrow O_4^-(H_2O)_2 + H_2O$	46.5[a]	0.482	This work
$O_6^-(H_2O) \rightarrow O_6^- + H_2O$	61.9[a]	0.642	This work

[a]The binding energy is derived from the thermochemical cycle, $D_0(AX^-) = EA(AX) + D_0(AX) - EA(A)$, where EA=electron affinity and D_0=dissociation energy. To a first approximation $D_0(AX) \approx 0$ so $D_0(AX^-) = EA(AX) - EA(A)$. Due to the approximate nature of calculation we do not assign absolute uncertainties.

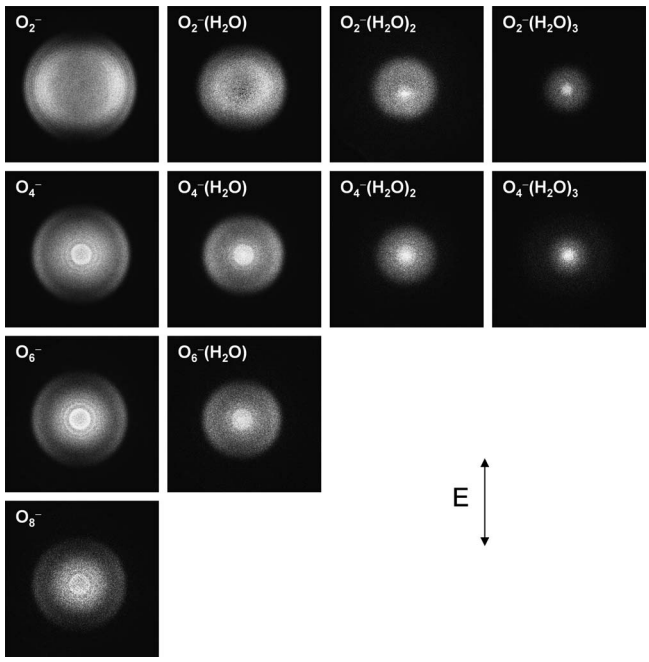

FIG. 1. 355 nm photoelectron images of $[O_{2n}(H_2O)_m]^-$, $n=1-4$, $m=0-3$. The double arrow indicates the direction of laser polarization. All images were recorded under the same conditions.

tionally unresolved bands.[2] The O_4^- ion has served as a model system for studying photodissociation dynamics.[6–9,11] Translational spectroscopy showed that fragments are produced with both high and low internal energies, with a complicated wavelength dependence of translational energy release.[8] Coincidence experiments, which looked at the neutral fragments and photoelectrons, revealed autodetachment from vibrationally excited O_2^- fragments formed from O_4^- and O_6^-.[9,12] Femtosecond studies of O_{2n}^- have been used to investigate the time-resolved aspects of the photodissociation, revealing two different time constants for the $n>2$ systems.[23] A fast direct component was found to produce vibrationally cold fragments, while a slow channel yielded internally excited fragments, presumed to arise from intramolecular vibrational-energy redistribution. The contribution of the fast, direct dissociation pathway was observed to decrease with increasing cluster size.[23] More recently, the infrared spectra of the O_{2n}^- clusters have been measured.[24] This work showed that two different isomers of the O_4^- core are noticeable in the O_6^- cluster due to different solvent binding motifs perturbing the core anion structure. However, the structures of these two different core anions could not be described.

A number of theoretical works have investigated the properties of solvated superoxide. A number of these studies focusing on the $O_2^-(H_2O)_m$ clusters[25,26] have indicated that water forms a single hydrogen bond with the O_2^- core, leaving a free O–H group, which tends to form hydrogen bonds with adjacent water molecules in the larger hydrates. This structural motif has been confirmed by gas-phase infrared spectroscopy.[22] Less attention has been paid by theorists to the O_{2n}^- series.[20,27] The only high-level study of O_4^- indicated that this anion has a D_{2h} ground-state geometry with a 1.998 Å distance between the two equivalent oxygen moieties.[20] For comparison, the $O_2^- \cdot \cdot HOH$ bond lengths in $O_2^-(H_2O)$ is calculated to be 1.702 Å.[26] The shorter bond length in hydrated superoxide compared to O_4^- reflects the relative magnitudes of the binding energies for the two clusters.

In this work, we report the photoelectron spectra and anionic photofragmentation pathways of the $[O_{2n}(H_2O)_m]^-$, $n=1-4$, $m=0-3$ clusters, highlighting the effects of heterogeneous versus homogenous solvation on the structural properties and photochemistry of the O_4^- anion. With core switching being rather common in cluster anions of varying size, we investigate the effects of solvation on the anionic cluster core in the extreme regime where solvent (water) binding energies are significantly larger than the core-anion's dissociation energy. Two different regimes can conceivably result from hydration of O_4^-. In one limit, hydration can be viewed as a perturbation to the core O_4^- anion, whose structural identity is preserved despite the strong solvation interactions. In the other extreme, the O_4^- core structure would break down, resulting in a cluster characterized as $O_2^-(O_2)_{n-1}(H_2O)_m$. Using a combination of photoelectron imaging spectroscopy and cluster photofragmentation, this work discriminates between these possible structural motifs. In addition, we observe electron autodetachment from O_2^- photofragments for some of the $[O_{2n}(H_2O)_m]^-$ clusters and discuss its implications to fragment excitation energy and the cluster fragmentation mechanism.

II. EXPERIMENTAL APPARATUS

The experiments are performed using a pulsed reflectron time-of-flight mass spectrometer equipped with a velocity-map[28] imaging detector for photoelectron imaging experiments, which has been described in detail previously.[29] Anions are generated via pulsed supersonic expansion of neat O_2, which is intersected by a 1 keV electron beam. Hydrated clusters are formed from ambient water vapor trapped in the gas manifold. The anions are accelerated to a kinetic energy of 3 keV and focused in the laser interaction

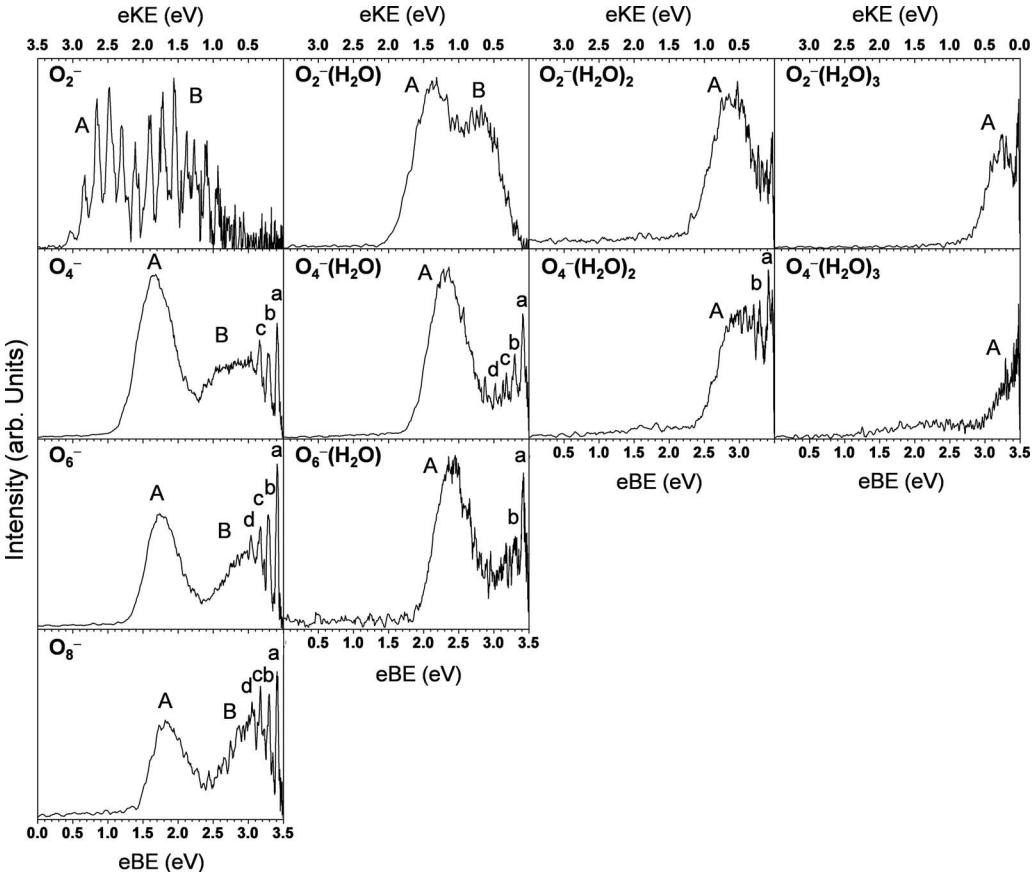

FIG. 2. Photoelectron spectra of $[O_{2n}(H_2O)_m]^-$, $n=1-4$, $m=0-3$ corresponding to the images shown in Fig. 1. For $n=1$, the major direct photodetachment bands labeled A and B correspond to the formation of O_2 in the $X\ ^3\Sigma_g^-$ and $a\ ^1\Delta_g$ electronic states. For $n\geq 2$, band A corresponds to dissociative photodetachment of O_4^- yielding $2O_2(X\ ^3\Sigma_g^-)+e^-$, while band B corresponds to $O_4^- \rightarrow O_2(X\ ^3\Sigma_g^-)+O_2(a\ ^1\Delta_g)+e^-$. The sharp peaks at low eKEs, attributed to O_2^- fragment autodetachment, are labeled a–d, in order of decreasing electron binding energy.

region, where the ion beam is crossed with a pulsed laser beam (355 nm, 8 ns, 25 mJ/pulse). The laser radiation is linearly polarized in the direction parallel to the imaging detector and is mildly focused by a 2 m focal length lens mounted 1.3 m before the ion interaction region. Parent ions are detected using an in-line microchannel plate (MCP) detector. Two types of experiments are performed in the laser interaction region: photoelectron imaging and photofragmentation.

Photoelectron images are recorded using the velocity-map[28] method. The photodetached electrons are projected on a 40 mm diameter position sensitive MCP detector (Burle, Inc.) using a static electric field defined by a series of electrodes.[30] Images are accumulated for $\sim 5\times 10^4$ experimental cycles using a 1 megapixel charged-coupled device (CCD) camera. A three dimensional reconstruction of the two dimensional images is performed using an inverse Abel transform as implemented in the BASEX program.[31] The well-known[14,32] photodetachment transitions of O^- and O_2^- are used for energy calibration of the resulting spectra.

Mass analysis of fragment ions is carried out using a linear-field reflectron with entrance and exit apertures. Typically, parent ions are initially refocused by the reflectron onto an off-axis MCP detector by optimizing the reflectron voltage V_p. Fragment ions are then focused on the same off-axis detector, with the same arrival time as the parent ions before, by setting the reflectron retarding potential to $V_f=V_p(m_f/m_p)$. The entire photofragment ion mass spectrum is recorded by scanning the reflectron potential.

III. RESULTS

A. Photoelectron imaging

The 355 nm photoelectron images of $[O_{2n}(H_2O)_m]^-$ are presented in Fig. 1. The corresponding spectra are shown in Fig. 2, with the observed band positions tabulated in Table II.

In the O_{2n}^- series, the overall features of the O_4^-, O_6^-, and O_8^- images are similar, the major difference being a decrease in the image size with increasing n, corresponding to increasing electron binding energies. The outer bands in the O_4^-, O_6^-, and O_8^- images display angular distributions similar to that of the O_2^- image, with maxima in the direction perpendicular to that of the laser polarization (Fig. 1). The perpendicular character of the photoelectron angular distributions is well understood for O_2^-, where photodetachment occurs from a $2p\pi_g^*$ orbital.[15]

The major bands in all photoelectron spectra shown in Fig. 2 are labeled with capital letters A and B, in the order of increasing binding energy. The resolved vibrational structure of bands A and B in the O_2^- spectrum, also discernable in the corresponding photoelectron image in Fig. 1, corresponds to the ground and first excited electronic states of O_2, the

TABLE II. Electron binding energies of the peak maxima of $[(O_2)_n(H_2O)_m]^-$ clusters at 355 nm.

	Band maximum (eV)					
Ion	A	B	a	b	c	d
O_2^-	1.022[a]	1.938[a]				
O_4^-	1.675	2.882	3.410	3.291	3.161	
O_6^-	1.789	3.032	3.413	3.286	3.166	3.036
O_8^-	1.886	3.050	3.411	3.297	3.171	3.054
$O_2^-(H_2O)$	2.142	2.847				
$O_4^-(H_2O)$	2.352	>3.495	3.412	3.298	3.176	3.023
$O_6^-(H_2O)$	2.431	>3.495	3.420	3.305		
$O_2^-(H_2O)_2$	2.905	3.450				
$O_4^-(H_2O)_2$	3.048	>3.495	3.412	3.291		
$O_2^-(H_2O)_3$	3.472	3.238				
$O_4^-(H_2O)_3$	>3.495					

[a]Vibrational peaks with maximum intensity for the $X\ ^3\Sigma_g^-$ and $a\ ^1\Delta_g$ photodetachment bands of O_2^-. These are not strictly vertical detachment energies, but the values are reasonable approximations.

$X\ ^3\Sigma_g^-$, and $a\ ^1\Delta_g$ states,[14] respectively. The higher-electron binding energy (eBE) wing of band B also most likely contains some contribution from the $O_2^- \rightarrow O_2(b\ ^1\Sigma_g^-)$ detachment channel. Following the work of Li *et al.*,[9] the vibrationally unresolved A and B bands in the O_4^-, O_6^-, and O_8^- spectra are attributed to dissociative photodetachment of the O_4^- cluster core. Band A corresponds to the formation of two $O_2(X\ ^3\Sigma_g^-)$ molecules, while band B corresponds to $O_2(X\ ^3\Sigma_g^-)+O_2(a\ ^1\Delta_g)$.

In the O_4^- spectrum, bands A and B are shifted by 0.65 eV to higher eBE, compared to O_2^-. The shift gives an estimate of the $O_4^- \rightarrow O_2(X\ ^3\Sigma_g^-)+O_2^-(X\ ^2\Pi_g)$ dissociation energy and its magnitude cannot be accounted for by the solvation interaction corresponding to an $O_2^- \cdot O_2$ cluster structure. Therefore, the bonding between the two O_2 moieties in O_4^- is weakly covalent in character, as discussed previously by others.[17,20,21] The spectra of O_6^- and O_8^- are similar to that of O_4^-, but with smaller relative shifts of the two photodetachment bands. These smaller shifts can be accounted for by electrostatic solvation interactions attributed to $O_4^-(O_2)_{n-2}$ structures. The loss of vibrational resolution in the O_4^-, O_6^-, and O_8^- spectra has been recognized as resulting from dissociative photodetachment, where photodetachment of the anion accesses a repulsive part of the neutral cluster potential energy surface.[11]

In addition to the two major transitions, for O_4^-, O_6^-, and O_8^-, we also observe series of well defined, isotropic rings near the image centers (see Fig. 1). These features correspond to sharp low-electron kinetic energy spectral peaks (Fig. 2) labeled with lower-case letters in order of decreasing binding energy. These features are attributed to autodetachment of vibrationally excited O_2^- photofragments (*vide infra*).[9]

The effect of water addition is perceptible from the images in the second through fourth columns of Fig. 1, where the image areas are progressively smaller compared to the unhydrated counterparts, corresponding to increasing electron binding energies. It also appears that the hydrated-anion images reveal increasingly isotropic angular distributions, although they retain their predominantly perpendicular character.

For $O_2^-(H_2O)$, the two partially overlapping bands A and B, assigned to two lowest electronic states of O_2,[12] are shifted to higher eBEs compared to the respective detachment transitions in O_2^-. The bands, however, appear to be closer in energy as a result of hydration. The difference in the A and B peak maxima in the $O_2^-(H_2O)$ spectrum in Fig, 2 is 0.705 eV, compared to the well established 0.9773 eV experimental term energy for the $a\ ^1\Delta_g$ state of O_2,[14] and the 0.915 eV difference between the $X\ ^3\Sigma_g^-$ and $a\ ^1\Delta_g$ band maxima in our O_2^- spectrum.

Each of the $O_4^-(H_2O)$ and $O_6^-(H_2O)$ spectra consists of a single band, shifted to higher eBE compared to band A in $O_2^-(H_2O)$, and perhaps just the onset of band B, whose maximum is now outside the accessible energy range. Several sharp low-electron kinetic energy (eKE) features are also evident both in the $O_4^-(H_2O)$ and $O_6^-(H_2O)$ images in Fig. 1 and the corresponding spectra in Fig. 2, Similar to the unhydrated O_4^-, O_6^-, and O_8^- ions, these features are attributed to autodetachment from O_2^- photofragments.

The addition of two and three waters further increases the electron binding energies, as seen in the third and fourth columns of Fig. 2. For $O_2^-(H_2O)_2$ and $O_2^-(H_2O)_3$, only a single major band, A, is clearly observed in each spectrum, while the onset of a second feature, B, may be discernable at eBEs near 3.5 eV. For $O_4^-(H_2O)_2$, the spectrum consists of a single band at high electron binding energy, with two low-eKE features (a and b) ascribed to O_2^- fragment autodetachment. Finally, the $O_4^-(H_2O)_3$ spectrum shows just the onset of band A.

B. Photofragmentation

Figure 3 shows the 355 nm photofragment mass spectra for the same mass-selected $[O_{2n}(H_2O)_m]^-$ parent ions as those studied above by photoelectron imaging. The photofragmentation yields predominantly O_2^- and $O_2^-(H_2O)_l (l<m)$ anionic products. In the $O_2^-(H_2O)_m$, $m=1-3$, series, fragmentation is observed for $O_2^-(H_2O)_2$ only, with O_2^- and $O_2^-(H_2O)$ products of nearly equal (very weak) intensity. This is in contrast to the O_{2n}^-, $n=2-4$, series, which gives O_2^- as the only, but very intense photofragment. The clusters with more

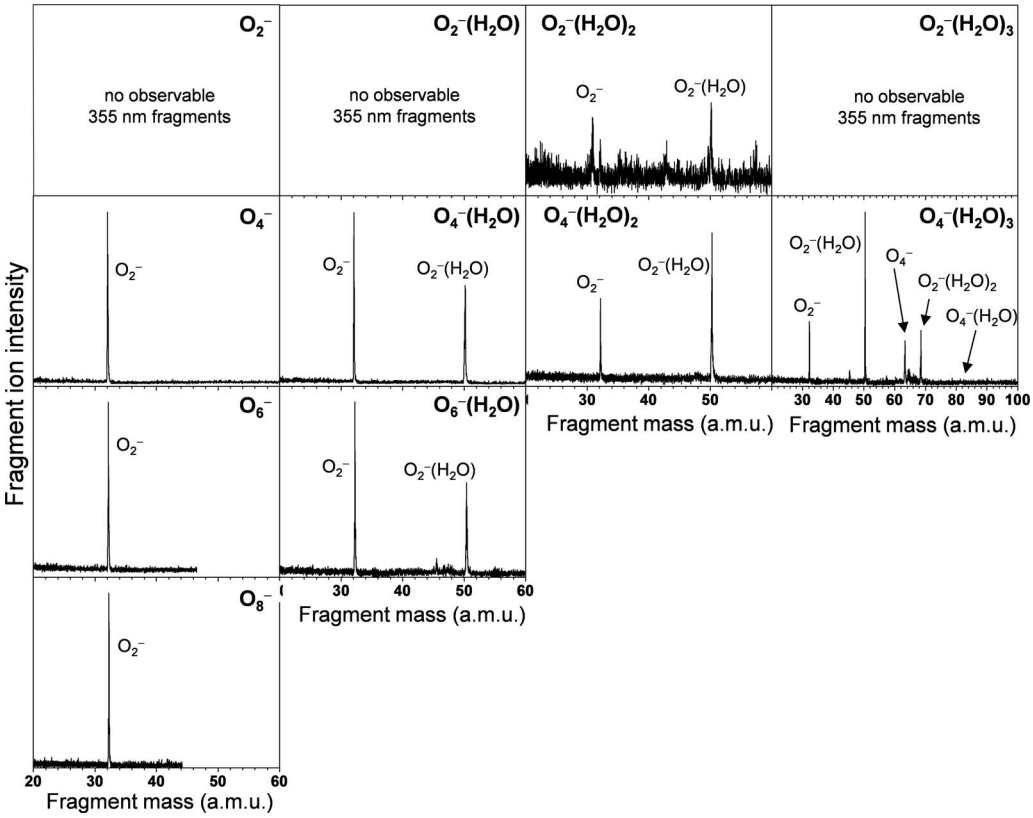

FIG. 3. 355 nm photofragmentation mass spectra for $[O_{2n}(H_2O)_m]^-$, $n=1-4$, $m=0-3$. No anionic photofragment signals were discerned for $O_2^-(H_2O)_n$, $n=0$, 1, and 3.

than one oxygen molecule and one or multiple waters yielded rich fragmentation spectra. For instance, the $O_4^-(H_2O)_m$, $m=1,2$ clusters produce O_2^- and $O_2^-(H_2O)$ as anionic photofragments. The relative intensity of the latter increases with increasing incremental hydration and for $O_4^-(H_2O)_3$ two higher-mass ions appear, O_4^- and $O_2^-(H_2O)_2$. For $O_6^-(H_2O)$, we again only observe two fragments, O_2^- and $O_2^-(H_2O)$, with relative intensities virtually identical to those measured for $O_4^-(H_2O)$.

IV. DISCUSSION

To put our observations in the context of past work, we open the discussion by comparing the present data to the previous results for the O_{2n}^- and $O_2^-(H_2O)_m$ cluster series. The photoelectron spectrum of O_2^- in Fig. 2 is in agreement with previously reported spectra.[14,15] The $O_2^-(H_2O)_m$ spectra also agree with the previous measurements at 388 and 258 nm.[12] Similarly, the spectra for O_4^-, O_6^-, and O_8^- in the first column of Fig. 2 are in good agreement with those reported previously,[9] except for the absence of the autodetachment peaks in the past spectra collected using a magnetic-bottle analyzer not equipped to observe these low-eKE transitions.[2] Further, our 355 nm fragmentation spectra of O_4^- to O_8^- are consistent with those previously reported at 1064 nm,[3] with the major difference being no O_4^- fragments observed in our case. This is likely due to the larger photon energy in our experiment. No photofragmentation spectra have been reported previously for the $O_{2n}^-(H_2O)_m$, n, $m \geq 1$ series at 355 nm.

The principal new findings of this work are summarized as follows. First, the O_4^- core anion is preserved not only in the O_{2n}^- clusters[2,9,12,20,21] but also in the hydrated $O_{2n}^-(H_2O)_m$, $n \geq 2$, species. This observation signifies that the weakly (covalently) bonded O_4^- core structure nonetheless withstands the strong hydration interactions. Second, isotropic low-eKE bands, characteristic of autodetachment from vibrationally excited O_2^- fragments, appear in the photofragmentation of not only O_4^- and O_6^- (Refs. 9 and 12) but also the hydrated $O_{2n}^-(H_2O)_m$, $n \geq 2$, clusters, as well as O_8^-. These bands provide a partial measure of the product state distributions resulting from cluster dissociation.

A. The O_4^- core anion

The first of the above conclusions—the persistence of the O_4^- core anion—is based on the overall shape of the photoelectron spectra in Fig. 2 and particularly the shifts of the direct-detachment photoelectron bands (A and B) quantified in Table II.

In the pure-oxygen clusters, the band shifts from O_2^- to O_4^- are significantly larger than those from O_4^- to O_6^- and from O_6^- to O_8^-. Apart from the solvation-induced shifts, the spectra of O_6^- and O_8^- are similar to that of O_4^-, consistent with an O_4^- core within the larger clusters. This view is further supported by the solvation energies listed in Table I. The photofragmentation spectra of O_{2n}^-, $n=2-4$, all reveal a single fragment, O_2^-, with no O^- or O_3^- fragments. This observation highlights the fact that the $O_4^- \rightarrow O_2^- + O_2$ dissociation energy, $D_0(O_4^-)=0.445$ eV,[18] while larger than that of

the larger oxygen clusters, e.g., $D_0(O_6^- \rightarrow O_4^- + O_2) = 0.109$,[18] is still much lower than the bond dissociation energy of O_2^-. These energetics are, in turn, consistent with the predicted D_{2h}-symmetry ground-state structure of O_4^-, with an O_2-O_2 distance of ~2 Å.[20] Thus, O_4^- may be viewed as a dimer anion consisting of two $O_2^{-1/2}$ units with a relatively weak covalent bond between them.

Anion hydration increases the electron detachment energy, as evidenced by the A and B band shifts in our data (Fig. 2 and Table II). For example, the approximately 1 eV difference between the vertical detachment energies of O_2^- and $O_2^-(H_2O)$ is consistent with the O_2^- hydration energy of 0.967 eV determined from threshold photodetachment studies.[12] The vibrational structure in the $O_2^-(H_2O)$ spectrum is lost due to hydration and the splitting between the $X\ ^3\Sigma_g^-$ and $a\ ^1\Delta_g$ states in oxygen is slightly smaller for $O_2(H_2O)$, based on our data, compared to bare O_2. Hydration of O_4^- and O_6^- leads to similar, albeit somewhat smaller, shifts (due the more delocalized nature of the excess electron in these ions, compared to O_2^-). The spectra of $O_4^-(H_2O)$ and $O_6^-(H_2O)$ in Fig. 2 are qualitatively similar to those of O_4^- and O_6^-, respectively, suggesting that an O_4^- core is preserved within these clusters. The dissociation or solvation energies in Table I are approximate because the ion structures are not clearly understood.

More accurate solvation energies would include the interactions between neutral solvent molecules, which are particularly important in the case of non-negligible water-water interactions.

B. Electron autodetachment from O_2^- photofragments

In addition to direct photodetachment bands A and B, the photoelectron spectra of pure-oxygen clusters O_{2n}^-, $n \geq 2$, as well as some of their hydrated counterparts, $O_{2n}^-(H_2O)_m$, display low-eKE features (peaks a–d in Fig. 2). The positions of these peaks do not shift as a result of solvation or hydration. In addition, these spectral features correspond to isotropic bands in the photoelectron images (Fig. 1), as expected for an indirect-detachment process. Therefore, these features are assigned to photoinduced autodetachment, namely, autodetachment from O_2^- photofragments. Similar features have been observed previously in experiments on O_4^- at 355 nm and O_6^- at 532 and 355 nm,[9] but no autodetachment has been reported for O_8^- or the hydrated $O_{2n}^-(H_2O)_m$, $n \geq 2$, clusters.

For bare O_2^-, autodetachment is expected for vibrational levels with $v \geq 4$, as these levels lie higher in energy than the ground electronic and vibrational state of neutral O_2.[2,9] The autodetachment arises from a breakdown of the Born–Oppenheimer approximation, where the vibrational excitation of the anion is transferred to electronic degrees of freedom, giving the excess electron sufficient energy to undergo a bound-free transition. The vibrational state distribution of the resulting neutral product is not expected to follow a typical Franck–Condon progression.[9] In our spectra we see no evidence of autodetachment to excited vibrational states of O_2 or from other ionic fragments. Assuming the O_2 is formed only in $v=0$, peaks a–d in Fig. 2 correspond to autodetachment from O_2^- fragments with $v=4-7$, respectively.

The conclusions derived from the photoelectron spectra in Fig. 2 are consistent with the photofragmentation data in Fig. 3. For the $O_4^-(H_2O)_m$ series, the O_2^- fragment decreases in relative intensity with increasing hydration and becomes a rather minor product for $O_4^-(H_2O)_3$. For $O_4^-(H_2O)$, O_2^- is the major observed photofragment *and* a series of O_2^- autodetachment features is prominent in the photoelectron spectrum, indicating that nascent O_2^- is formed in vibrational levels both below and above $v=4$. In contrast, for $O_4^-(H_2O)_3$, plenty of O_2^- based photofragments are formed, but the O_2^- autodetachment signal is relatively weak, suggesting that the fragments are produced with predominantly $v<4$. Therefore, while O_2^- photofragments in the smaller clusters are formed with considerable internal energy, hydration provides alternative pathways for the flow of excess energy.

The $O_2^-(H_2O)$ ion shows no indication of fragment autodetachment (Fig. 2), consistent with no anionic photofragments being observed for this parent ion in Fig. 3. On the other hand, the very weak photofragment signal seen in Fig. 3 for the $O_2^-(H_2O)_2$ parent anion is consistent with the weak autodetachment feature in the corresponding image in Fig. 2. No photofragments were seen for the $O_2^-(H_2O)_3$ parent ion. This is consistent with the small parent-cluster intensity in the experiment, but may also indicate that the observed autodetachment is the dominant decay mechanism for the corresponding excited clusters. This would not be surprising if the transient excited state corresponded to the excess electron being transferred to the water network.

C. Cluster energetics and autodetachment

Thus, the combination of photofragmentation and autodetachment results provides a gauge of internal energy distributions of nascent O_2^- photofragments. The differences in H_2O and O_2 solvent binding energies to superoxide are nearly equal to the differences in vertical electron binding energies reported in Table II. Similarly, we can estimate the binding energies of H_2O and O_2 to O_4^- as the differences in electron binding energies in the corresponding photoelectron spectra. As these data show, water binding energies are consistently larger than oxygen binding energies (Table I). Therefore, upon cluster fragmentation, water molecule loss removes more excess energy than oxygen molecule loss.

The relative energetics of anion hydration and solvation by O_2 are illustrated in Fig. 4 on the examples of O_8^- (left) and $O_4^-(H_2O)_3$ (right). The schematic diagram, based on our experimental solvation and hydration energy values, shows that the removal of all three water molecules from $O_4^-(H_2O)_3$ uses up a sizable fraction of the total of 3.5 eV available from 355 nm photon absorption. The additional energy needed for $O_4^- \rightarrow O_2^- + O_2$ dissociation plus the O_2^- vibrational excitation corresponding to the $v=4$ level (0.541 eV),[14] as required for the autodetachment, puts us close to the available energy limit indicated in Fig. 4. The loss of oxygen molecules in O_8^- removes a smaller fraction of the total energy, and hence the resulting anionic fragments are produced with greater average vibrational excitation.

These results are in agreement with the time-resolved (femtosecond) studies of O_{2n}^- clusters.[23] These studies indi-

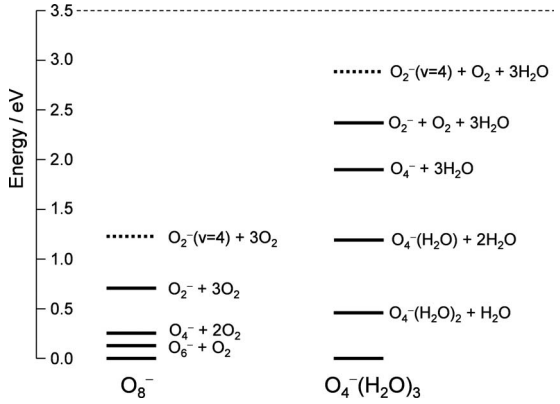

FIG. 4. Schematic energy level diagram representing the fragmentation of O_8^- and $O_4^-(H_2O)_3$ to form O_2^- fragments in $v=0$ and $v=4$. The solvation energies corresponding to H_2O and O_2 solvent loss are from Table I. The dashed horizontal line at 3.5 eV represents the total energy available following the absorption of a 355 nm photon.

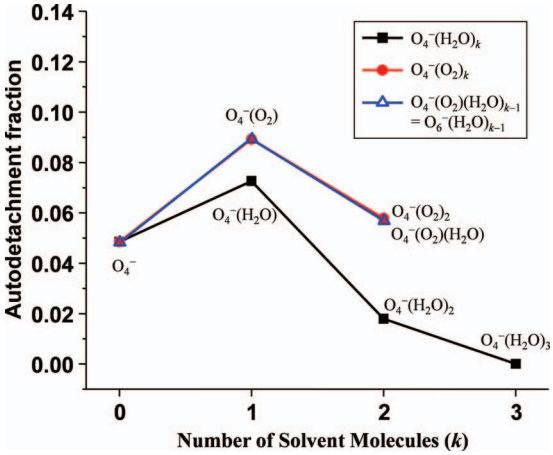

FIG. 5. The autodetachment fraction A, calculated as the overall fragment autodetachment intensity relative to the total photoelectron signal for a given cluster anion, as defined in Eq. (1), plotted as a function of the number of solvent molecules k. Because of the overlap between the autodetachment peaks and the direct-detachment bands, the plotted ratio is only an approximate guide. The near overlap of the $O_4^-(H_2O)_2$ and $O_4^-(O_2)(H_2O)$ data points reflects a real trend deduced from the data. See the text for details.

cated that dissociation rates for the larger clusters are dominated by a slow component, resulting from the excess energy being randomly distributed among the vibrational degrees of freedom, while the smaller clusters dissociate quickly, via a direct pathway. A simple Franck–Condon analysis shows that the vibrational excitation on the O_2^- fragments imparted in direct O_4^- dissociation is rather small ($v<4$, on average), compared to a statistical process in the larger clusters. These considerations are consistent with the observed increase in intensity of O_2^- fragment autodetachment in progressing from O_4^- to O_6^-.

Additional analysis can be performed using the observed relative photoelectron cross sections. We define the autodetachment fraction A, calculated as the overall fragment autodetachment intensity relative to the total photoelectron signal observed for a given cluster anion,

$$A = \sigma_{\text{autodetach}}/(\sigma_{\text{autodetach}} + \sigma_{\text{photodetach}}). \quad (1)$$

Here, $\sigma_{\text{autodetach}}$ and $\sigma_{\text{photodetach}}$ are the relative autodetachment and direct photodetachment cross sections, respectively, determined by integrating the intensities of the corresponding transitions in Fig. 2. Because of the overlap between the autodetachment peaks and the direct-detachment bands, only very approximate ratio values could be calculated from the data; the results of this crude analysis do, however, provide the desired insight.

The approximate autodetachment fractions, as defined by Eq. (1), are plotted in Fig. 5 versus the number of solvent molecules for different-cluster types studied. In this analysis, we regard O_4^- as the core anion in all clusters studied, with the exception of the O_2^- based species. Then, the number of solvent molecules (k) in $O_4^-(H_2O)_m$ equals m, while for O_{2n}^-, described as $O_4^-(O_2)_{n-2}$, the solvation number is calculated as $k=n-2$. Finally, for $O_6^-(H_2O)_m$, viewed as $O_4^-(O_2)(H_2O)_m$, is $k=m+1$.

The resulting $A(k)$ trends are expected to reflect the varying degrees of fragment excitation for parent clusters of different sizes because only the excited ($v \geq 4$)O_2^- fragments can undergo autodetachment. Were the fragment vibrational excitation always dictated by random energy redistribution, one would expect the degree of excitation and, therefore, $A(k)$ to decrease monotonically with increasing k due to the increasing number of degrees of freedom available for energy partitioning. To the contrary, we find that the autodetachment fraction *increases* with the addition of a first solvent molecule (O_2 or H_2O) to the O_4^- core and only then, with additional solvation, shows the expected decrease.

We attribute the departure of this experimental observation from the statistical model prediction to the breakdown of two model assumptions. First, we caution that the $A(k)$ values reflect the true autodetachment trends only if one assumes that $\sigma_{\text{photodetach}}$ is approximately constant for all cluster sizes. In reality, one cannot expect direct photodetachment to be unaffected by solvation. Solvation is known to suppress photodetachment, favoring anionic photofragmentation channels instead. This has been demonstrated, for example, in our group's work on solvent-mediated reactivity of the $(CO_2)_n^-(H_2O)_m$ clusters.[29,33,34] The expected decrease in $\sigma_{\text{photodetach}}$ with increasing cluster size will tend to increase the fraction defined by Eq. (1), thus competing with the monotonic decrease expected from the statistical model.

Second, the assumption of statistical energy redistribution is not applicable to all molecular anions and small clusters. As discussed above, photodissociation of O_4^- has a fast channel yielding vibrationally cold O_2^-, in addition to a slow channel forming vibrationally excited O_2^-.[8,9] As the fast, cold O_2^- channel is important in unsolvated O_4^-, the fragment autodetachment yield for this anion should be smaller than dictated by statistical considerations, effectively decreasing the autodetachment fraction for unsolvated O_4^- in Fig. 5.

Thus, the observed trends are qualitatively consistent with the statistical predictions, but only if one overlooks the results for unsolvated O_4^-. It appears that solvation of O_4^- by either O_2 or H_2O serves to increase fragmentation via the slow (indirect) dissociation channel. This pathway allows for energy redistribution within the clusters, giving rise to more

excited O_2^- photofragments and therefore increasing the relative yield of fragment autodetachment. Additional solvent molecules, on the other hand, increase the number of degrees of freedom available for energy redistributions, causing the degree of fragment excitation and, therefore, the autodetachment yield to decrease accordingly.

D. Structures of $[O_{2n}(H_2O)_m]^-$ clusters

Finally, we summarize the implications of these results to the structures of $[O_{2n}(H_2O)_m]^-$ clusters. For the pure-oxygen cluster anions, we suggested that oxygen molecules solvate an O_4^- core, in agreement with the past conclusions, for example by Kelley *et al.*[17] The dissociation energy of this core anion is smaller than the typical energy of anion hydration. We also must take into account that the binding energy of water molecules to O_2^- is larger than to O_4^- due to the more localized charge distribution in the former case. It is therefore conceivable *a priori* that upon hydration the $[O_{2n}(H_2O)_m]^-$ clusters would form around a unique O_2^- molecule, with strong hydrogen bonds to one or more of the water molecules, while any additional oxygen molecules might be considered as spectators within the cluster. A similar dimer-to-monomer anion core switching has been discussed in the case of heterogeneous $(CO_2)_n^-(H_2O)_m$ clusters.[29,34]

However, the strong intensities of the O_2^- and $O_2^-(H_2O)$ photofragments observed in the $[O_{2n}(H_2O)_m]^-$ case, combined with the structure of the corresponding photoelectron spectra, argue in favor of a preserved O_4^- core. Upon photon absorption, this core is promoted to an excited state correlating with the $O_2^-+O_2$ dissociation fragments. The photoelectron images of the $[O_{2n}(H_2O)_m]^-$ clusters appear very similar to those of O_{2n}^-, suggesting a common anionic core in both cases, even though the core is likely to be perturbed by the strong hydration interactions in the presence of water molecules. Although infrared spectroscopy of O_6^- indicated two core structures for O_4^-,[24] the energetic difference between the structures may be difficult to resolve in the photoelectron imaging experiment.

V. CONCLUSIONS

We investigated the photochemistry of $[O_{2n}(H_2O)_m]^-$ clusters at 355 nm using photoelectron imaging and photofragment mass spectroscopy. The results show that both pure-oxygen and hydrated clusters with $n \geq 2$ form an O_4^- core anion with two weakly (yet covalently) bound $O_2^{-1/2}$ moieties. All clusters studied can be therefore described in terms of the $O_4^-(H_2O)_m(O_2)_{n-2}$ structures. Fragmentation of these cluster anions yields predominantly O_2^- and $O_2^-(H_2O)_l$, $l<m$, anionic products. The O_2^- autodetachment features in photoelectron images reveal that the fragments are vibrationally excited. Upon solvation of an O_4^- cluster core, the autodetachment yield increases relative to overall photoelectron signal upon the addition of a first solvent molecule (O_2 or H_2O), but then decreases with the addition of a second. The initial increase is attributed, in part, to the increased contribution of the indirect (statistical) core dissociation channel in the solvated anion that yields vibrationally excited fragments. The subsequent decrease is due to the increasing energy bath associated with an extended solvent network available for statistical redistribution of excess energy.

ACKNOWLEDGMENTS

We are grateful to Professor Richard Mabbs (Washington University, St. Luis) for his comments on the draft of this manuscript. This work is supported by the National Science Foundation (Grant No. CHE-0713880).

[1] L. A. Posey, M. J. DeLuca, and M. A. Johnson, Chem. Phys. Lett. **131**, 170 (1986).
[2] M. J. DeLuca, C.-C. Han, and M. A. Johnson, J. Chem. Phys. **93**, 268 (1990).
[3] C. C. Han and M. A. Johnson, Chem. Phys. Lett. **189**, 460 (1992).
[4] M. A. Buntine, D. J. Lavrich, C. E. Dessent, M. G. Scarton, and M. A. Johnson, Chem. Phys. Lett. **216**, 471 (1993); C. R. Sherwood and R. E. Continetti, *ibid.* **258**, 171 (1996).
[5] D. J. Lavrich, M. A. Buntine, D. Serxner, and M. A. Johnson, J. Phys. Chem. **99**, 8453 (1995).
[6] C. R. Sherwood, M. C. Garner, K. A. Hanold, K. M. Strong, and R. E. Continetti, J. Chem. Phys. **102**, 6949 (1995).
[7] K. A. Hanold, M. C. Garner, and R. E. Continetti, Phys. Rev. Lett. **77**, 3335 (1996).
[8] C. R. Sherwood, K. A. Hanold, M. C. Garner, K. M. Strong, and R. E. Continetti, J. Chem. Phys. **105**, 10803 (1996).
[9] R. J. Li, K. A. Hanold, M. C. Garner, A. K. Luong, and R. E. Continetti, Faraday Discuss. **108**, 115 (1997).
[10] K. A. Hanold, A. K. Luong, and R. E. Continetti, J. Chem. Phys. **109**, 9215 (1998); T. G. Clements and R. E. Continetti, Phys. Rev. Lett. **89**, 033005 (2002).
[11] K. A. Hanold and R. E. Continetti, Chem. Phys. **239**, 493 (1998).
[12] A. K. Luong, T. G. Clements, M. S. Resat, and R. E. Continetti, J. Chem. Phys. **114**, 3449 (2001).
[13] S. A. Corcelli, J. A. Kelley, J. C. Tully, and M. A. Johnson, J. Phys. Chem. A **106**, 4872 (2002).
[14] K. M. Ervin, W. Anusiewicz, P. Skurski, J. Simons, and W. C. Lineberger, J. Phys. Chem. A **107**, 8521 (2003).
[15] F. A. Akin, L. K. Schirra, and A. Sanov, J. Phys. Chem. A **110**, 8031 (2006).
[16] M. Arshadi and P. Kebarle, J. Phys. Chem. **74**, 1483 (1970).
[17] J. A. Kelley, W. H. Robertson, and M. A. Johnson, Chem. Phys. Lett. **362**, 255 (2002).
[18] K. Hiraoka, J. Chem. Phys. **89**, 3190 (1988).
[19] N. G. Adams, D. K. Bohme, D. B. Dunkin, F. C. Fehsenfeld, and E. E. Ferguson, J. Chem. Phys. **52**, 3133 (1970).
[20] A. J. A. Aquino, P. R. Taylor, and S. P. Walch, J. Chem. Phys. **114**, 3010 (2001).
[21] D. C. Conway, J. Chem. Phys. **50**, 3864 (1969).
[22] J. M. Weber, J. A. Kelley, W. H. Robertson, and M. A. Johnson, J. Chem. Phys. **114**, 2698 (2001).
[23] D. H. Paik, N. J. Kim, and A. H. Zewail, J. Chem. Phys. **118**, 6923 (2003); D. H. Paik, T. M. Bernhardt, N. J. Kim, and A. H. Zewail, *ibid.* **115**, 612 (2001).
[24] J. C. Bopp, A. N. Alexandrova, B. M. Elliott, T. Herden, and M. A. Johnson, Int. J. Mass Spectrom. **283**, 94 (2009).
[25] E. M. C. Robinson, W. L. Holstein, G. M. Stewart, and M. A. Buntine, Phys. Chem. Chem. Phys. **1**, 3961 (1999); I. F. W. Kuo and D. J. Tobias, J. Phys. Chem. A **106**, 10969 (2002); H. M. Lee and K. S. Kim, Mol. Phys. **100**, 875 (2002); T. Seta, M. Yamamoto, M. Nishioka, and M. Sadakata, J. Phys. Chem. A **107**, 962 (2003); A. J. Bell and T. G. Wright, Phys. Chem. Chem. Phys. **6**, 4385 (2004); V. Y. Antonchenko and E. S. Kryachko, Chem. Phys. **327**, 485 (2006).
[26] V. Y. Antonchenko and E. S. Kryachko, J. Phys. Chem. A **109**, 3052 (2005).
[27] G. V. Chertihin and L. Andrews, J. Chem. Phys. **108**, 6404 (1998).
[28] A. Eppink and D. H. Parker, Rev. Sci. Instrum. **68**, 3477 (1997).
[29] L. Velarde, T. Habteyes, and A. Sanov, J. Chem. Phys. **125**, 114303 (2006).
[30] E. Surber and A. Sanov, J. Chem. Phys. **116**, 5921 (2002); E. Surber, R. Mabbs, and A. Sanov, J. Phys. Chem. A **107**, 8215 (2003).

[31] V. Dribinski, A. Ossadtchi, V. A. Mandelshtam, and H. Reisler, Rev. Sci. Instrum. **73**, 2634 (2002).
[32] S. J. Cavanagh, S. T. Gibson, M. N. Gale, C. J. Dedman, E. H. Roberts, and B. R. Lewis, Phys. Rev. A **76**, 052708 (2007).
[33] T. Habteyes, L. Velarde, and A. Sanov, Chem. Phys. Lett. **424**, 268 (2006).
[34] R. Mabbs, E. Surber, L. Velarde, and A. Sanov, J. Chem. Phys. **120**, 5148 (2004).